Environmental Science & Technology

Article

pubs.acs.org/est

Pulmonary Surfactant Suppressed Phenanthrene Adsorption on Carbon Nanotubes through Solubilization and Competition As Examined by Passive Dosing Technique

Jian Zhao,[†,‡] Zhenyu Wang,*[,†] Hamid Mashayekhi,[‡] Philipp Mayer,[§] Benny Chefetz,[∥] and Baoshan Xing*[,‡]

[†]College of Environmental Science and Engineering, Ocean University of China, Qingdao 266100, China

[‡]Department of Plant, Soil and Insect Sciences, University of Massachusetts, Amherst, Massachusetts 01003, United States

[§]Department of Environmental Science, Aarhus University, P.O. Box 358, 4000 Roskilde, Denmark

[∥]Department of Soil and water Sciences, Hebrew University of Jerusalem, Rehovot 76100, Israel

Supporting Information

ABSTRACT: Adsorption of phenanthrene on carbon nanotubes (CNTs) was examined in the presence of pulmonary surfactant (Curosurf) and its main components, dipalmitoyl phosphatidylcholine (DPPC) and bovine serum albumin (BSA). A passive-dosing method based on equilibrium partitioning from a preloaded polymer was successfully employed to measure phenanthrene binding and speciation at controlled freely dissolved concentrations while avoiding phase separation steps. Curosurf, DPPC, and BSA could all linearly solubilize phenanthrene, and phenanthrene solubilization by Curosurf was 4 times higher than individual components (DPPC or BSA). In the presence of Curosurf, DPPC or BSA, adsorption of phenanthrene by multiwalled CNTs (MWCNTs) was suppressed, showing competitive adsorption between pulmonary surfactant (or DPPC, BSA) and phenanthrene. Competitive adsorption between Curosurf and phenanthrene was the strongest. Therefore, when phenanthrene-adsorbed CNTs enter the respiratory tract, phenanthrene can be desorbed due to both solubilization and competition. The bioaccessibility of phenanthrene adsorbed on three MWCNTs in the respiratory tract would be positively related to the size of their outer diameters. Moreover, the contribution of solubilization and competition to desorption of phenanthrene from MWCNTs was successfully separated for the first time. These findings demonstrate the two mechanisms on how pulmonary surfactants can enhance desorption and thus possibly biological absorption of phenanthrene adsorbed on CNTs.

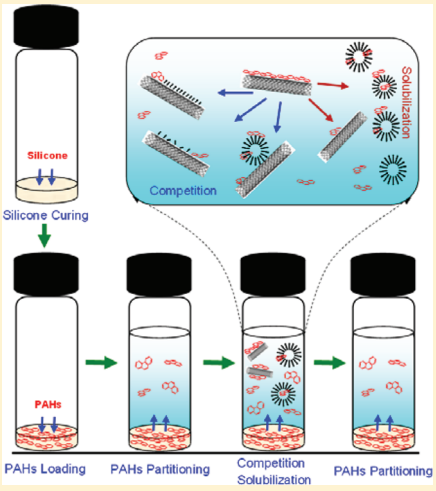

INTRODUCTION

The respiratory tract is considered one of the major entrances for carbon nanotubes (CNTs) into the human body because of their relative low density and asbestos-like properties.[1,2] When inhaled by human or animals, CNTs could induce adverse effects such as lung inflammation and cardiovascular effects.[3,4] Before entering alveolar cells and exhibiting toxicity, CNTs initially encounter pulmonary surfactant which covers the thin aqueous lining layer. Pulmonary surfactant is formed by type II alveolar cells and consists of lipids (approximately 90%, mainly phospholipids) and proteins (10%).[5] CNTs in the atmosphere may contain polycyclic aromatic hydrocarbons (PAHs) because PAHs are good carbon sources for CNTs synthesis in the arc discharge method[6] and an important byproduct in the catalytic chemical vapor deposition method with thermal treatment.[7] CNTs could also accumulate PAHs in the atmosphere due to their high adsorption affinity and capacity.[8] Thus the concern is that the adsorbed PAHs may be released from the inhaled CNTs when they are in contact with pulmonary surfactant. Our previous study observed that 60−90% of phenanthrene were released from MWCNTs in the gastrointestinal fluids, which further increases the health concern.[9] Until now, the behavior and bioavailability of adsorbed PAHs on CNTs in the respiratory tract were still unknown.

Simulated lung fluid has been used to evaluate the bioaccessibility of metals in fly ash[10] and mine waste.[11] The organic components of these simulated lung fluids were acetate salts, citrate salts, glycine, and/or albumin. These types of simulated lung fluids may not be appropriate for assessing the bioaccessibility of hydrophobic PAHs on CNTs because these simulated organic components are not remarkably surface-

Received: December 13, 2011
Revised: April 17, 2012
Accepted: April 20, 2012
Published: April 20, 2012

active, and the release of PAHs from CNTs depends on their solubilization.[9] Davies and Feddah modified the simulated lung fluid by adding one component of pulmonary surfactant (dipalmitoyl phosphatidylcholine, DPPC).[12] The dissolution of aerosol particles in the modified lung fluid was then highly increased. Actually, pulmonary surfactant is highly surface-active and DPPC is the main surfactant component (~50%) responsible for the surface tension reduction in the respiratory tract.[13] Hence, it is essential to investigate the effects of pulmonary surfactant on PAHs adsorption by CNTs.

Traditionally, adsorption experiments in aqueous phase use a batch/centrifugation method.[14,15] This method requires the complete separation of adsorbent and adsorbate. Pulmonary surfactant cannot be separated from the aqueous phase using centrifugation because of its complicated compositions. Therefore, in this study a passive dosing method avoiding centrifugation was employed to investigate the effects of pulmonary surfactant on PAHs adsorption by and desorption from CNTs. Passive dosing is the inverse of passive sampling (e.g., solid phase microextraction), and it is based on the equilibrium partitioning of analytes (e.g., PAHs) from a preloaded silicone and into an aqueous solution or suspension. This results in tightly controlled freely dissolved concentrations of the analytes (C_{free}) and allows speciation, binding, and sorption to be deduced from the measured total concentration in the solution.[16,17] The solubilization (sorption) of PAHs by pulmonary surfactant can be calculated by the difference between total PAHs concentration in the solution and C_{free}. In our previous study, adsorption of phenanthrene by CNTs was suppressed by the biomolecules (e.g., pepsin) in the simulated gastrointestinal fluids due to competitive adsorption and solubility enhancement,[9] whereas the exact contribution of each could not be determined using the traditional batch/centrifugation method. Hence, we intended to separate the contribution of each using the passive dosing method in this study.

Therefore, in this study, we employed a commercially available pulmonary surfactant (Curosurf) to investigate the effects of pulmonary surfactant on phenanthrene (a model PAH) adsorption by CNTs. The role of pulmonary surfactant components, DPPC, and bovine serum albumin (BSA, replacement for surfactant proteins) were further studied. The contribution of competitive adsorption and solubility enhancement during the desorption process was also quantitatively evaluated in this study.

MATERIALS AND METHODS

Materials. Silastic MDX4−4210 Elastomer kit for poly(dimethylsiloxane) (PDMS) silicone preparation was obtained from Dow Corning corporation. Because of the similar compositions to human pulmonary surfactants,[18] Curosurf (Chiesi Pharmaceutici, Parma, Italy) was chosen and used as pulmonary surfactant in this work. Curosurf extracted from porcine lungs is a commercial pulmonary surfactant containing lipids and proteins (Supporting Information (SI) Table S1). DPPC, 1,2-dioleoyl-sn-glycero-3-phosphocholine (DOPC) and 1,2-dipalmitoyl-sn-glycero-3-phospho-(1′-rac-glycerol) (sodium salt) (DPPG) were obtained from Avanti Polar Lipids (Alabaster, AL). BSA powder was purchased from Sigma Aldrich. ^{14}C labeled (8.2 μCi/μmol) and unlabeled phenanthrene was purchased from Sigma-Aldrich Chemical Co. The molecular weight, molecular volume, water solubility (37 °C) and octanol−water partition coefficient (log K_{ow}) of phenanthrene are 178.2 g/mol, 169.5 Å^3, 1.75 mg/L and 4.57, respectively.[9,15] Three multiwalled carbon nanotubes (MWCNTs) with different outer diameters (MWCNT20, MWCNT40, and MWCNT60) were used as adsorbents. They were purchased from Shenzhen Nanotech Port Co., China and used after acid purification[19] and their characteristics are listed in SI Table S2.

Passive Dosing Vials Preparation. The MDX4-4210 kit contains a PDMS silicone prepolymer and a catalyst. Prepolymer and catalyst (10:1, w/w) were mixed according to the product instructions. Passive dosing vials were prepared using the method of Birch et al.[16] Briefly, 600 ± 5 mg of the silicone mixture were added to each 20 mL vial, and the vials were then sealed and placed into the refrigerator (4 °C) for 48 h to eliminate bubbles in the PDMS. Then the vials were left to cure at room temperature for 72 h and 110 °C in an oven for another 48 h. After curing, the silicone was cleaned three times with methanol (HPLC grade, Fisher) (each time at least 12 h) to remove impurities and oligomers, followed by rinsing three times with ultrapure water to remove the methanol. The cleaning procedure was conducted at 37 °C, the same temperature to the following sorption experiments. The vials were wiped with lint-free tissue after the cleaning procedure.

Loading of Passive Dosing Vials. ^{14}C-labled phenanthrene was added in methanol to obtain a radioactive phenanthrene solution with a final concentration of 5 mg/L. Phenanthrene stock solution (2005 mg/L) was prepared by dissolving the unlabeled phenanthrene in the radioactive phenanthrene solution. The stock solution was then diluted sequentially to a series of concentrations (20−2005 mg/L) using radioactive phenanthrene solution. These phenanthrene solutions with different concentrations (800 μL) were added to different passive dosing vials, and 500 μL and 1 mL of ultrapure water were then added to each vial at 30 min intervals to promote the phenanthrene partitioning from methanol to silicone. Overnight, 17.7 mL ultrapure water was added into the vials and all vials were shaken at 37 °C for 72 h. The solution was removed from the vial and the vials were wiped with lint-free tissue. To eliminate the influence of the remaining methanol in the silicone, the loaded vials were amended by 20 mL ultrapure water and shaken at 37 °C for 24 h to reach equilibrium,[16,20] this procedure was repeated until the C_{free} in the water after equilibration was constant (SI Figure S1). C_{free} in each procedure was measured by adding 1 mL solution into 4 mL Ultima Gold XR cocktail (Perkin-Elmer) for liquid scintillation counting (Beckman LS6500). Phenanthrene concentration in the silicone ($C_{silicone}$) was calculated by the mass difference. Finally, the water was removed and the loaded vials with different phenanthrene amounts were obtained.

Solubilization Experiments in the Passive Dosing Vials. The Curosurf stock suspension (80 mg/mL) was diluted to obtain a Curosurf solution of 40 mg/L with background solution. The background solution was a physiological saline (NaCl, 0.9%) with 200 mg/L NaN_3 to avoid the degradation of phenanthrene and other solutes (e.g., Curosurf) dissolved inside. DPPC, DOPC, and DPPG were suspended in background solution by ultrasonicating (42 kHz, 100 W, 20 ± 2 °C) for 40 min, and then diluted to a series of solutions. DPPC-BSA solution was prepared by adding BSA powder to DPPC solution. For the solubilization experiment, 20 mL Curosurf or lipids solutions was added to each phenanthrene-loaded vial and shaken at 37 °C for 5 days to reach equilibrium (SI Figure S2). Then the whole solution was transferred to

another vial and the total phenanthrene concentration in the solution (C_{total}) was measured. During the partition/sorption process, silicone in the vial did not significantly adsorb Curosurf, DPPC or BSA, thus, the aqueous phase concentration of Curosurf, DPPC or BSA was not changed in the vials (SI Figure S3). The vials were then quickly rinsed five times with background solution and wiped with lint-free tissue. Background solution (20 mL) was then equilibrated in these vials and the measured concentrations in these solutions were used as a surrogate for the C_{free}. This measured C_{free} was also the equilibrium aqueous concentration during the solubilization experiment. For phenanthrene at a given C_{free} (0.087 mg/L), solubilization by Curosurf, DPPC or BSA at different concentrations (2−200 mg/L) was also determined. Even at 200 mg/L, pulmonary surfactants had no influence on the measurement of ^{14}C-labeled phenanthrene (SI Figure S4). To further study and compare the solubilization effect of the pulmonary surfactant components, solubilization of phenanthrene by DPPC (40 mg/L), DOPC (40 mg/L), DPPG (40 mg/L), or their mixtures (each component at 40 mg/L) was also determined at a given C_{free} (0.087 ± 0.004 mg/L).

Adsorption Experiments. The passive dosing vials loaded with phenanthrene were used to conduct the adsorption of phenanthrene on MWCNTs. First, 20 mL of background, Curosurf (40 mg/L), DPPC (40 mg/L) or DPPC-BSA (40 mg/L DPPC, 4 mg/L BSA) solution was added to the loaded vials which contained 1.00 mg MWCNTs (MWCNT20, MWCNT40 or MWCNT60). All vials were shaken at 37 °C for 5 days to reach equilibrium. The solution in each vial was then moved to another vial. Initially, some MWCMTs may still have remained on the inner wall or silicone surface of older vial. The wall and silicone were rinsed carefully using the removed solution to ensure the entire solution including all MWCNTs was transferred. After that, background solution (20 mL) was amended into the older vial and the C_{free} in the background solution was measured. The solutions in the new vials were ultrasonicated (42 kHz, 100 W, 20 ± 2 °C) for 1 h to suspend the MWCNTs. C_{total} was measured by adding 1 mL suspension into 4 mL Ultima Gold XR cocktail for liquid scintillation counting. For MWCNTs in the Curosurf, DPPC and DPPC-BSA solutions, C_{total} here includes (i) free phenanthrene in the solution (C_{free}), (ii) phenanthrene concentration solubilized by Curosurf, DPPC, and/or BSA ($C_{solubilized}$), and (iii) phenanthrene adsorbed on MWCNTs ($C_{adsorbed}$). Therefore, the equilibrium concentration of adsorbed phenanthrene on MWCNTs (q_e) was determined by mass difference: $q_e = (C_{total} - C_{solubilized} - C_{free})/C_{CNT}$. In the experiment, the measurement of radioactive phenanthrene was not influenced by the presence of Curosurf, DPPC, BSA, or MWCNTs, and MWCNTs could be sufficiently suspended by ultrasonication (42 kHz, 100 W, 20 ± 2 °C) (SI Figure S5). The adsorption of phenanthrene on MWCNTs in the background solution was also conducted using the batch/centrifugation method, and the nearly overlapping between sorption isotherms obtained by the two methods was observed (SI Figure S6).

Statistical Analysis. All experiments were run in triplicate. The sorption of PAHs by surfactant was likely a partitioning process,[21] so phenanthrene sorption by pulmonary surfactants was fitted by a linear model (eq 1). Nonlinear Freundlich (eq 2), Langmuir (eq 3) and Dubinin-Ashtakhov (DA, eq 4) models[8,22] were employed to fit the data of phenanthrene adsorption on MWCNTs which have heterogeneous site-energy distribution. The bioaccessibility of MWCNTs-adsorbed phenanthrene and the contribution of solubilization in the pulmonary surfactant solutions were calculated using the fitting results of these models.

$$q_e = KC_{free} \quad (1)$$

$$q_e = K_f C_{free}^{\ n} \quad (2)$$

$$q_e = Q^0 C_{free}/(K_L + C_{free}) \quad (3)$$

$$q_e = \frac{Q^0}{10^{(\varepsilon/E)^b}} \quad (4)$$

where q_e (mg/kg) is the equilibrium adsorbed concentration of solute; C_{free} (mg/L) is the equilibrium aqueous concentration (also the freely dissolved concentration) of solute; K [L/kg] is the partition coefficient; K_f [(mg/kg)/(mg/L)^n] is the Freundlich affinity coefficient, and n is the Freundlich exponential coefficient; Q^0 (mg/kg) is the saturated adsorption capacity; K_L (mg/L) is the Langmuir affinity coefficient; ε (kJ/mol) = $-RT\ln(C_{free}/C_s)$ is the effective adsorption potential, where C_s (mg/L) is the water solubility of solute, R [8.314 × 10^{-3} kJ/(mol K)] and T (K) are universal gas constant and absolute temperature, respectively; E (kJ/mol) is the "correlating divisor" and b is a fitting parameter.

RESULTS AND DISCUSSION

Passive Dosing in the Adsorption Experiments. Varying the loaded amount of phenanthrene, a wide range of freely dissolved concentrations were successfully established and maintained by passive dosing (Figure S7). The good fitting of linear equation (r^2=0.999) indicated that the loading from methanol to silicone and the release from silicone to water were efficient and reproducible, and both steps were strictly partitioning processes. The C_{free} in the adsorption experiments are often in a narrow range and much lower than the water solubility using the batch/centrifugation method[8] because of the high adsorption capacity of CNTs and low water solubility of phenanthrene. Recently, Kah et al. employed a depletive passive sampling method[23] using polyoxymethylene to determine PAHs sorption to CNTs at extremely low aqueous equilibrium concentrations (pg/L level), but not at high concentrations because of high PAHs adsorption on CNTs and partitioning in polyoxymethylene. For the passive dosing method in this study, a concentration range of C_{free}s from the low microgram per liter range to almost solubility was easily and precisely obtained by loading the silicone with different concentrations of phenanthrene. The silicone to water partition ratio ($K_{silicone,\ water} = C_{silicone}/C_{free}$) governed the partitioning of phenanthrene in the passive dosing vials. It was in the present study determined to be 4470 L/kg (or 5030 L/L) at 37 °C (Figure 1), which is in good agreement with a reported value of 5160 L/L that was obtained for a different silicone material but at the same temperature.[24] The high $K_{silicone,\ water}$ value was the basis for this passive dosing method and for the very limited depletion of phenanthrene from silicone during sequential incubations.[17] The passive dosing vials could thus be used several times without affecting the sorption data due to the high loading of phenanthrene in PDMS.

Solubilization Effect of Pulmonary Surfactant. Phenanthrene was highly solubilized in the Curosurf solution (40 mg/L) (Figure 2A). Curosurf is a natural pulmonary surfactant extracted from porcine and is composed of lipids (mainly

dx.doi.org/10.1021/es2044773 | Environ. Sci. Technol. 2012, 46, 5369−5377

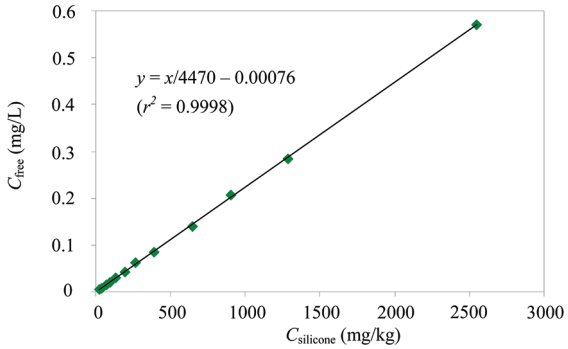

Figure 1. Preparation of passive dosing vials with different concentrations of free phenanthrene. The relationship between concentration of free phenanthrene in water after equilibration (C_{free}) and phenanthrene concentration in silicone ($C_{silicone}$) after equilibration is linear.

DPPC) and proteins. DPPC, BSA and the mixture of DPPC and BSA were used to simulate the components of pulmonary surfactant. Although DPPC is the main component of Curosurf, its solubilization effect at 40 mg/L was much lower, indicating that other components of Curosurf may also play a key role in phenanthrene solubilization. BSA at 40 mg/L exhibited the lowest solubilization in comparison to other components. Solubilization of phenanthrene in the solutions was caused by the sorption of phenanthrene by the surface-active solutes such as Curosurf, DPPC and BSA.

The sorption isotherms of phenanthrene by these solutes are displayed in Figure 2B. All isotherms were fitted well with both Linear and Freundlich models (SI Table S3). The good fitting of Linear model indicated that pulmonary surfactants in the solutions acted as favorable media for phenanthrene partitioning. The partition coefficients (K) of phenanthrene between the test compounds and water followed an order: Curosurf > DPPC > DPPC-C1 > DPPC-C2 > BSA. Phospholipid molecules such as DPPC were mainly in the form of vesicles in water as prepared by ultrasonication.[25] The average hydrodynamic size of the DPPC vesicles in the background solution was around 340 nm (SI Figure S8). The partition coefficient of DPPC vesicles ($\log K_{DPPC}$) at 37 °C was 4.00. Although there is no report on $\log K_{DPPC}$ of PAHs at 37 °C, the relationship between $\log K_{DPPC}$ and $\log K_{ow}$ was examined for chlorobenzenes.[26] Using this relationship and the $\log K_{ow}$ of phenanthrene (4.57), the calculated $\log K_{DPPC}$ values at 27 and 43 °C were 2.76 and 4.06, respectively, in agreement with the value obtained at 37 °C in our study. With the addition of BSA (4 and 40 mg/L), the sorption of phenanthrene on DPPC was decreased (Figure 2B). This observation may be explained as follows: (i) the aggregation of DPPC vesicles was enhanced in the presence of BSA.[27] Such aggregation could contribute to the reduction of available sites for phenanthrene sorption; (ii) the hydrophobic sites of both DPPC and BSA monomer molecules may also be reduced as a result of the interaction between DPPC and BSA. The higher solubilization of Curosurf than DPPC and DPPC-BSA suggested that Curosurf would be a better model of pulmonary surfactant in solubilization study. Other lipid components in Curosurf may be responsible for the higher solubilization of pulmonary surfactants. In addition to DPPC (the major component), unsaturated phosphatidylcholine and phosphatidylglycerol make up ~25% and ~10% of total lipids, respectively. DOPC (an unsaturated phosphatidylcholine) and DPPG (a phosphatidylglycerol) were therefore

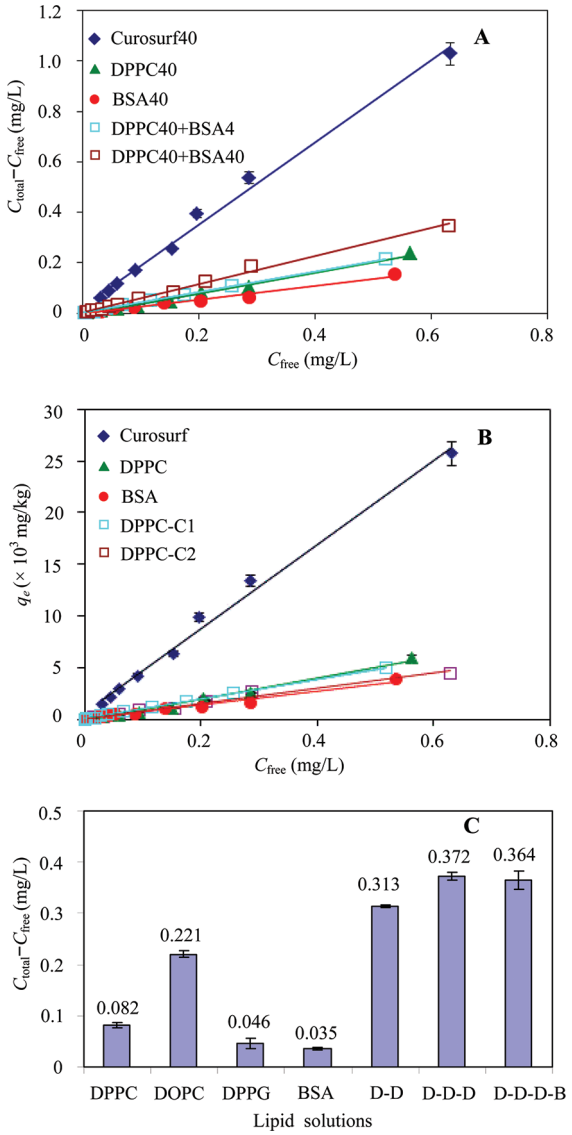

Figure 2. Solubilization (A) and sorption (B) of phenanthrene in 40 mg/L Curosurf (Curosurf40), 40 mg/L DPPC (DPPC40), 40 mg/L BSA (BSA40), 40 mg/L DPPC with the addition of 4 or 40 mg/L BSA (DPPC40+BSA4, DPPC40+BSA40) solutions, and the solubilization of phenanthrene by different lipid compositions (C) at a given C_{free} (0.087 mg/L) using passive dosing vials. In panels A and C, C_{total} is the phenanthrene concentration in the solution after equilibrium, "$C_{total}-C_{free}$" is the solubilized phenanthrene concentration. In panel B, DPPC-C1 and DPPC-C2 are the phenanthrene sorption by DPPC in the "DPPC40+BSA4" and "DPPC40+BSA40" solutions. In panel C, for all tested solutions, the concentration of each component was 40 mg/L, "D-D", "D-D-D", and "D-D-D-B" represent the mixtures of "DPPC and DOPC";"DPPC, DOPC, and DPPG"; and "DPPC, DOPC, DPPG, and BSA" respectively.

selected to further study the solubilization of phenanthrene by the pulmonary surfactant components.[18,28] As shown in Figure 2C, DOPC had higher solubilization enhancement than DPPC and DPPG. The phase state of the lipids is expected to influence the solubilization capacity.[29] DPPC at 37 °C is in the gel state, whereas the DOPC is in the liquid crystalline state.[26] Phospholipid molecules in the liquid crystalline phase were loosely distributed and could result not only in the higher fluidity of the lipid molecules but also in better penetration of hydrophobic organic compounds.[26,29] Therefore, the solubiliza-

dx.doi.org/10.1021/es2044773 | Environ. Sci. Technol. 2012, 46, 5369–5377

tion is greater for lipids in the liquid crystalline state (DOPC) as compared to the gel state (DPPC). For the lipid mixture (DPPC-DOPC or DPPC-DOPC-DPPG), the solubilization effect of the lipid mixture was higher than the sum of the respective effects of the mixture components. This result could also be explained by the phase state as reported by Yamamoto and Liljestrand,[26] in which the DPPC-DOPC mixture was in the liquid crystalline state. To our knowledge, this is the first study to apply passive dosing in solubilization/adsorption studies at a range of analyte concentrations.

Phenanthrene Adsorption on MWCNTs in the Presence of Pulmonary Surfactants. The adsorption isotherms of phenanthrene on MWCNTs are presented in Figure 3. Three nonlinear adsorption models were used to fit the adsorption data of CNTs. The discussion below was mainly based on the fitting results of DA model (Table 1) because of its higher r_{adj}^2 (>0.996) than that of Freundlich (SI Table S4) and Langmuir (SI Table S5) models. The Polanyi theory-based DA model is widely applied in the adsorption of hydrophobic organic contaminants,[8,21] and also fitted the phenanthrene adsorption on MWCNTs well in this study. Polanyi theory works for adsorption on inhomogeneous surface. For MWCNTs, the origin of heterogeneity is from sorption site energy distribution among external surface, groove area, interstitial pore, inner cavity, interwall spaces, and intrinsic defects of the side walls. In the DA model equation, the adsorption potential ε ($\varepsilon = -RT \ln(C_{free}/C_s)$) is the required energy from the adsorption sites to the locations outside the attractive force field of the solid surface. For a certain adsorbate at a constant temperature, ε is dependent on C_{free}. However, when the solution contains another adsorbate which could solubilize the first adsorbate, the DA model cannot be applied to fit the adsorption isotherms because of the unavailable data on C_{free} when using the batch/centrifugation method. In contrast, C_{free} could be obtained using the passive dosing method in this study and DA model was applied to fit the adsorption data of phenanthrene adsorption in the presence of Curosurf. As described in the Materials and Methods section, in the Curosurf solution, the directly adsorbed concentration on MWCNTs was calculated as $q_e = (C_{total} - C_{solubilized} - C_{free})/C_{CNT}$, where $C_{solubilized}$ was calculated from the phenanthrene isotherm of Curosurf in Figure 2B.

The DA model fitted adsorption capacity (Q^0) of investigated MWCNTs in the background and Curosurf solutions has the order of MWCNT20 > MWCNT40 > MWCNT60 (Table 1). The surface area normalized adsorption capacity (Q^0/A_{surf}) follows the same order. For MWCNTs, the adsorption sites for PAHs were mainly on external surface rather than the inner cavities or interwall surface.[30] MWCNT20 with the smallest outer diameters (SI Table S2) had the largest external surface area, thus showing the highest amounts of available surface sites for phenanthrene. Micropores on the external surface may constitute an important portion of the total sites as indicated by the positive relationship between Q^0/V_{micro} and Q^0/A_{surf} (Table 1), which also agrees with the reported results.[15] This is because micropores are the high-energy sites for phenanthrene adsorption compared to the regular sites on the external surface,[30] and the surface area from micropores contributes a high portion of total MWCNTs surface area. In addition, Curosurf did not significantly suspend MWCNTs as compared to the background solution. For all MWCNTs, Q^0 value in the Curosurf solution was lower than that in the background solution, indicating the competitive

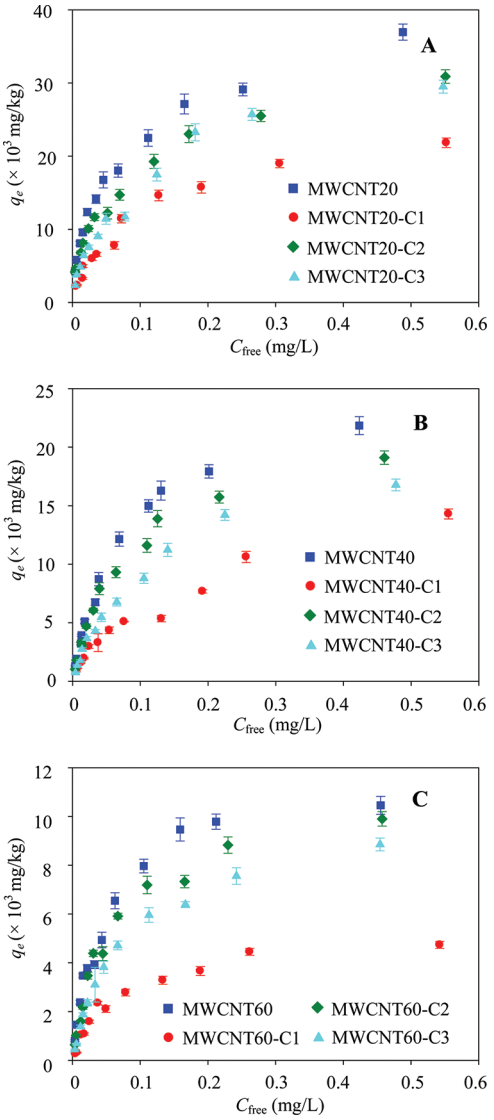

Figure 3. Adsorption of phenanthrene on MWCNT20 (A), MWCNT40 (B), and MWCNT60 (C) in background, Curosurf (40 mg/L), DPPC (40 mg/L), and DPPC-BSA (40, 4 mg/L) solutions. In panel A, "MWCNT20-C1", "MWCNT20-C2", and "MWCNT20-C3" are the adsorption of phenanthrene on MWCNT20 in the presence of Curosurf, DPPC and DPPC-BSA, respectively, the same to panels B and C. In Curosurf, DPPC or DPPC-BSA solution, the equilibrium adsorbed concentration on MWCNTs was calculated using the following eqution: $q_e = (C_{total} - C_{solubilized} - C_{free})/C_{CNT}$, where C_{total}, C_{free} were the total and free phenanthrene in the solution, $C_{solubilized}$ was calculated by the isotherm of phenanthrene by Curosurf, DPPC or DPPC-BSA in Figure 2B, C_{CNT} was the concentration of MWCNTs in the solution.

adsorption between phenanthrene and the components of Curosurf on the MWCNTs surface. Surfactants such as bile salts[9] and cetylpyridinium[21] were observed as competitors of PAHs as indicated by the increased linearity of isotherms in the previous studies. Hence, the increased n value in the presence of Curosurf (significantly increased for MWCNT20 ($p = 0.018$) and MWCNT40 ($p = 0.003$); insignificantly for MWCNT60 ($p = 0.426$)) further demonstrated the occurrence of competitive adsorption (SI Table S4). Pulmonary surfactant is a complex mixture of approximately 90% lipids (mainly DPPC) and 10% proteins.[31,32] Therefore, DPPC (40 mg/L) and DPPC-BSA (40

dx.doi.org/10.1021/es2044773 | Environ. Sci. Technol. 2012, 46, 5369−5377

Table 1. Fitting Results of Sorption Isotherms of Phenanthrene on MWCNTs in Curosurf, DPPC and DPPC-BSA Solutions by Dubinin-Ashtakhov (DA) Model

		parameters					
adsorbent	solution	Q^0 (× 10^3 mg/kg)	b	E (KJ/mol)	Q^0/A_{surf}[a] (mg/m^2)	Q^0/V_{micro}[a] (mg/cm^3)	r_{adj}^2[b]
MWCNT20	water[c]	41.5 ± 1.1	1.70 ± 0.11	16.0	0.330	814	0.996
	Curosurf	28.5 ± 1.2	1.51 ± 0.24	13.6	0.226	558	0.975
	DPPC	40.3 ± 1.1	1.34 ± 0.12	15.8	0.320	791	0.992
	DPPC-BSA	40.1 ± 1.2	1.45 ± 0.19	13.8	0.318	785	0.984
MWCNT40	water	26.8 ± 1.1	2.00 ± 0.14	13.8	0.311	787	0.995
	Curosurf	18.0 ± 1.1	1.49 ± 0.14	12.4	0.209	529	0.992
	DPPC	22.1 ± 1.1	2.01 ± 0.17	13.1	0.257	649	0.985
	DPPC-BSA	20.5 ± 1.1	1.86 ± 0.18	12.9	0.239	604	0.989
MWCNT60	water	11.6 ± 1.1	2.38 ± 0.25	15.4	0.158	398	0.982
	Curosurf	4.64 ± 0.06	2.84 ± 0.33	14.6	0.0636	160	0.974
	DPPC	10.7 ± 1.1	2.36 ± 0.23	14.5	0.146	368	0.984
	DPPC-BSA	9.47 ± 1.03	2.29 ± 0.06	14.2	0.130	327	0.996

[a] Q^0/A_{surf} and Q^0/V_{micro} are the surface area (A_{surf}) and micropores volume (V_{micro}) normalized Q^0, respectively. [b] r_{adj}^2 is the adjusted coefficient of determination and it is influenced by both the number of data points (m) and the number of fitting parameters (p). $r_{adj}^2 = 1-(m-1)(1-r^2)/(m-p-1)$; [c] Water is the background solution.

and 4 mg/L) were used to further investigate the competitive sorption between phenanthrene and Curosurf components on MWCNTs (Figure 3). Similar to Curosurf, DPPC also decreased the Q^0 values of all MWCNTs (40.3, 22.1, and 10.7 mg/g for MWCNT20, MWCNT40, and MWCNT60, respectively), but still much higher than the Q^0 values in the Curosurf solution. This is probably because only one pulmonary surfactant components competed with phenanthrene on MWCNTs. In Curosurf solution, more sorption sites on MWCNTs suitable for phenanthrene could be occupied by other components of pulmonary surfactants such as DOPC, DPPG and protein. With the addition of another component (BSA), the competitive sorption was slightly stronger as indicated by the lower Q^0 (40.1, 20.5, and 9.47 mg/g for MWCNT20, MWCNT40, and MWCNT60, respectively) (Table 1). To further study the competitive sorption between phenanthrene and pulmonary surfactants, we employed DPPC to illustrate the MWCNT-pulmonary surfactant interactions. There were five possible conformations for DPPC molecules on the MWCNTs surface: (i) DPPC monomer molecules, (ii) cylindrical micelles, (iii) hemimicelles, (iv) bilayers, and (v) vesicles (SI) Figure S9. When adsorbed on hydrophobic MWCNTs surface, the bilayers of vesicles could be disrupted.[13,33] Moreover, it was observed that DPPC molecules wrapped around the carbon nanotubes were in the form of cylindrical micelles rather than hemimicelles using molecular dynamics simulation.[34] Therefore, DPPC molecules on the MWCNTs surface could be mainly in the form of DPPC monomer molecules or cylindrical micelles via hydrophobic interaction, and phenanthrene molecules could be partially replaced from the hydrophobic sites and released to the solution. Sorption of DPPC vesicles on MWCNTs may be not important due to the hydrophobic surface of MWCNTs and hydrophilic surface of DPPC vesicles in this work. However, sorption of vesicles could be higher on certain MWCNTs surface with more oxygen-containing functional groups (e.g., carboxylated MWCNTs).

Besides the direct adsorption, phenanthrene could be also indirectly adsorbed on MWCNTs by association with the Curosurf on MWCNTs. The adsorbed amount of Curosurf on MWCNTs is a key point to evaluate the indirect phenanthrene adsorption on MWCNTs. However, the adsorbed Curosurf amount was not available because the Curosurf could not be completely separated from MWCNTs (SI Figure S10). Bile salts and pepsin which are also amphoteric biomolecules and produced in the human body were used to estimate Curosurf sorption on MWCNTs. The saturated adsorption capacities of bile salts and pepsin on MWCNTs were in a range of 50−100 mg/g.[9] If the adsorbed Curosurf concentration on MWCNTs was assumed to be as high as 100 mg/g, there would be approximately 35 mg/L Curosurf remaining in the solution. Even after adsorption, Curosurf (35 mg/L) were still be able to highly solubilize phenanthrene (SI Figure S11) due to the low critical micelle concentration (CMC) (CMC of DPPC, 0.34 μg/L).[35] The calculated Q^0 values using DA model fitting results were then 31.0, 24.3, and 6.89 mg/g for MWCNT20, MWCNT40, and MWCNT60, respectively, still lower than the Q^0 values in the background solution (41.5, 26.8, and 11.6 mg/g for MWCNT20, MWCNT40, and MWCNT60, respectively). The decrease of Q^0 values indicates that phenanthrene could be desorbed and released into respiratory tracts if the phenanthrene-adsorbed MWCNTs are inhaled.

Bioaccessibility of Phenanthrene on MWCNTs in Simulated Respiratory Tract and the Contribution of Solubilization and Competition. When the phenanthrene-adsorbed MWCNTs enter respiratory tracts, phenanthrene could be partly desorbed from MWCNTs, which is defined as the bioaccessible fraction. In our experiment, the readily bioaccessible fraction for the respiratory tract includes the free phenanthrene and solublized phenanthrene by pulmonary surfactant. At a fixed C_{free}, the bioaccessibility of phenanthrene adsorbed on MWCNTs was calculated as bioaccessibility (%) = $(C_{free} + C_{solubilized})/C_{total} \times 100$, where $C_{solubilized}$ and $C_{adsorbed}$ were calculated by the Linear model (SI Table S3) and DA model fitting results (Table 1), respectively. In the Curosurf solution, the bioaccessibility followed an order: MWCNT60 > MWCNT40 > MWCNT20 (Figure 4A), which was negatively related to the order of the surface area of MWCNTs. The same bioaccessibility order was observed in the DPPC solution (Figure 4B) for different MWCNTs. For a given MWCNT,

dx.doi.org/10.1021/es2044773 | Environ. Sci. Technol. 2012, 46, 5369−5377

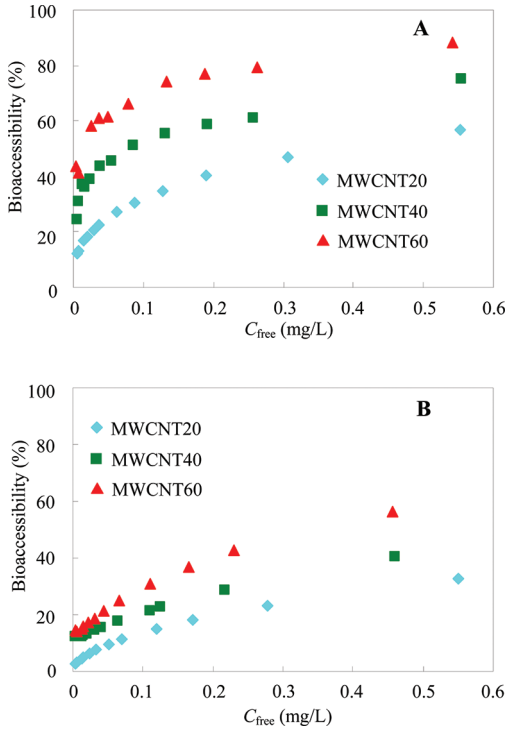

Figure 4. Bioaccessibility of MWCNTs-adsorbed phenanthrene in the Curosurf (A) and DPPC (B) solutions. When phenanthrene-adsorbed MWCNTs enter the respiratory tract, the released phenanthrene includes free phenanthrene (C_{free}) and solubilized phenanthrene ($C_{solubilized}$). In the passive dosing vials, at a fixed C_{free}, $C_{solubilized}$, and $C_{adsorbed}$ were calculated by the Linear model (SI Table S3) and DA model fitting results (Table 1) respectively. Bioaccessibility was calculated as the percentage of the amounts of free phenanthrene and solubilized phenanthrene to the total phenanthrene amount. Bioaccessibility (%) = $(C_{free} + C_{solubilized})/C_{total} \times 100$.

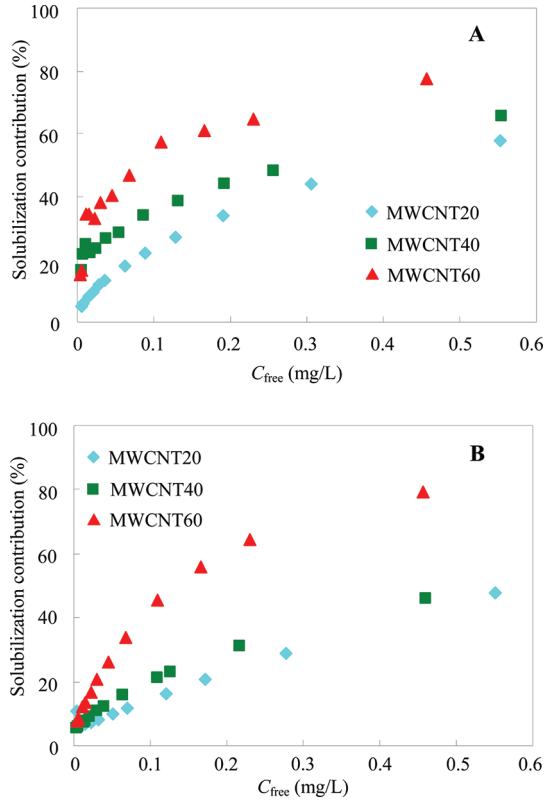

Figure 5. The contribution of solubilization to the desorbed phenanthrene amount from MWCNTs in 40 mg/L Curosurf (A) and DPPC (B) solutions. The desorbed phenanthrene amount here included the phenanthrene released from MWCNTs by solubilization and by competition with Curosurf or DPPC. At a fixed C_{free}, the contribution of solubilization was calculated using the following equation: Solubilization contribution (%) = $C_{solubilized}/(C_{solubilized}+C_{competed}) \times 100$. The solubilized phenanthrene amount in the Curosurf/DPPC solutions ($C_{solubilized}$) was obtained from the Linear model fitting results (SI Table S3) while the phenanthrene amount replaced by Curosurf/DPPC ($C_{competed}$) was the difference between the MWCNTs-adsorbed phenanthrene amounts in background solution and Curosurf/DPPC solution. The adsorbed phenanthrene amount was calculated by the DA model fitting results (Table 1).

phenanthrene bioaccessibility in the DPPC solution was lower than that in the Curosurf solution, due to the lower solubilization enhancement (Figure 2A) and competitive effect (Figure 3) of DPPC relative to Curosurf.

The contribution of solubilization enhancement and competitive effect to desorption of phenanthrene from MWCNTs as a function of Curosurf/DPPC concentration was further studied. At a fixed C_{free}, the solubilized phenanthrene amount in the Curosurf/DPPC solutions was obtained from the Linear model fitting results (SI Table S3) while the phenanthrene amount replaced by Curosurf/DPPC was the difference between the MWCNTs-adsorbed phenanthrene amounts in background solution and Curosurf/DPPC solution. At low C_{free}, Curosurf/DPPC tended to replace phenanthrene from the MWCNTs rather than solubilize phenanthrene (Figure 5). The contribution of solubilization increased with the increased C_{free} as a result of the decreasing available sites for competition. For different MWCNTs, the solubilization contribution followed the order of MWCNT60 > MWCNT40 > MWCNT20 in both Curosurf and DPPC solutions. MWCNT60 had the smallest surface sites to be occupied, and the amount of competition could be lowest. It is noted that if Curosurf/DPPC was adsorbed on MWCNTs, the contribution of solubilization in Figure 5 should be lower because of the overestimation of solubilization by Curosurf/DPPC. To our knowledge, this is the first report investigating the separation of solubilization and competition in an adsorption−desorption study. Besides pulmonary surfactant, other organic compounds such as natural organic matter and protein could also solubilize and compete with PAHs when adsorbing to CNTs.[9,36,37] Generally, solubilization and competition are present in any bisolute system. By separating the contribution of each, we could better understand the behavior of PAHs and other emerging organic contaminants at the CNTs-water interface in natural and biological systems.

Environmental Implication. We successfully examined the adsorption of phenanthrene by CNTs in pulmonary surfactant solutions using the passive dosing technique. From this study, passive dosing technique provides a possibility to study the sorption of PAHs in the complicated systems such as natural water and biological fluids when (i) the sorbent is soluble in the aqueous phase; (ii) the sorbent is difficult to be separated by centrifugation; and (iii) in the presence of two or more sorbents.

Besides the synthesis processes,[38] CNTs can be also released to air during the application and disposal. Based on actual information of product life-cycles, about 5% of CNTs in

dx.doi.org/10.1021/es2044773 | Environ. Sci. Technol. 2012, 46, 5369−5377

consumer products (e.g., plastics, sporting equipment) are released to air though most CNTs are bound into material matrix.[39] During waste incineration, it was assumed that 25% of CNTs became airborne.[39] Another study reported that the commercially available CNTs contained as high as 150 μg/g CNTs of total PAHs.[40] Therefore, the bioaccessibility of PAHs on PAHs−CNTs complexes is of importance in assessing the CNTs environmental and health risk. From this study, the adsorption of phenanthrene was highly suppressed by pulmonary surfactants due to both solubilization enhancement and competitive effect, suggesting PAHs could be readily desorbed from CNTs when PAHs−CNTs complexes enter the respiratory tract. The real concentration of pulmonary surfactants covering the alveoli is much higher than the tested concentration (40 mg/L) in this study. Therefore, the bioaccessibility of PAHs (e.g., phenanthrene) in the respiratory tract would be higher than that in our study. Moreover, after reaching other systems such as blood circulation, more PAHs could be desorbed and become bioaccessible, indicating health risk of PAHs-associated CNTs in addition to the toxicity of CNTs themselves.[3,4]

■ ASSOCIATED CONTENT

Supporting Information

Components of Curosurf (Table S1); Properties of carbon nanotubes (Table S2); Concentration of free phenanthrene after several times of partitioning equilibration (Figure S1); Equilibrium time of phenanthrene adsorption on MWCNTs (Figure S2); Effect of silicone on the aqueous phase concentration of Curosurf, DPPC or BSA (Figure S3); Influence of Curosurf, DPPC, BSA, and MWCNTs on the phenanthrene measurement (Figures S4 and S5); Adsorption experiments using batch/centrifugation and passive dosing methods (Figure S6); The relationship between $C_{methanol}$ and C_{free} (Figure S7); Linear and Freundlich model fitting results of sorption isotherms (Table S3); Average size of DPPC vesicles (Figure S8); Fitting results of sorption isotherms of phenanthrene on carbon nanotubes in the background, Curosurf, DPPC and DPPC-BSA solutions by Freundlich and Langmuir models (Tables S4 and S5); Possible schematic diagram for DPPC molecules on MWCNTs (Figure S9); Percentage of Curosurf in the supernatant after centrifugation (Figure S10); Phenanthrene solubilization by different concentrations of Curosurf and DPPC (Figure S11). This material is available free of charge via the Internet at http://pubs.acs.org.

■ AUTHOR INFORMATION

Corresponding Author

*Phone: +1 413 545 5212; fax: +1 413 545 3958; e-mail: bx@pssci.umass.edu (B.X.); e-mail: wang0628@ouc.edu.cn (Z.W.).

Notes

The authors declare no competing financial interest.

■ ACKNOWLEDGMENTS

This research was supported by National Natural Science Foundation of China (41073067, 41120134004), BARD (IS-4353-10), and USDA-AFRI Hatch program (MAS 00978).

■ REFERENCES

(1) Poland, C. A.; Duffin, R.; Kinloch, I.; Maynard, A.; Wallace, W. A. H.; Seaton, A.; Stone, V.; Brown, S.; MacNee, W.; Donaldson, K. Carbon nanotubes introduced into the abdominal cavity of mice show asbestos-like pathogenicity in a pilot study. *Nat. Nanotechnol.* **2008**, *3*, 423−428.

(2) Schleh, C.; Hohlfeld, J. M. Interaction of nanoparticles with the pulmonary surfactant system. *Inhal. Toxicol.* **2009**, *21*, 97−103.

(3) Li, Z.; Hulderman, T.; Salmen, R.; Chapman, R.; Leonard, S. S.; Young, S.; Shvedova, A.; Luster, M. I.; Simeonova, P. P. Cardiovascular effects of pulmonary exposure to single-wall carbon nanotubes. . *Environ. Health Perspect.* **2007**, *115*, 377−382.

(4) Muller, J.; Huaux, F.; Moreau, N.; Misson, P.; Heilier, J.; Delos, M.; Arras, M.; Fonseca, A.; Nagy, J. B.; Lison, D. Respiratory toxicity of multi-wall carbon nanotubes. *Toxicol. Appl. Pharmacol.* **2005**, *207*, 221−231.

(5) Schulze, C.; Schaefer, U. F.; Ruge, C. A.; Wohlleben, W.; Lehr, C. Interaction of metal oxide nanoparticles with lung surfactant protein A. *Eur. J. Pharm. Biopharm.* **2011**, *77*, 376−383.

(6) Lai, H. J.; Lin, M. C. C.; Yang, M. H.; Li, A. K. Synthesis of carbon nanotubes using polycyclic aromatic hydrocarbons as carbon sources in an arc discharge. *Mater. Sci. Eng., C* **2001**, *16*, 23−26.

(7) Plata, D. L.; Hart, A. J.; Reddy, C. M.; Gschwend, P. M. Early evaluation of potential environmental impacts of carbon nanotube synthesis by chemical vapor deposition. *Environ. Sci. Technol.* **2009**, *43*, 8367−8373.

(8) Yang, K.; Xing, B. Adsorption of organic compounds by carbon nanomaterials in aqueous phase: Polanyi theory and its application. *Chem. Rev.* **2010**, *110*, 5989−6008.

(9) Wang, Z. Y.; Zhao, J.; Song, L.; Mashayekhi, H.; Chefetz, B.; Xing, B. Adsorption and desorption of phenanthrene on carbon nanotubes in simulated gastrointestinal fluids. *Environ. Sci. Technol.* **2011**, *45*, 6018−6024.

(10) Twining, J.; McGlinn, P.; Loi, E.; Smith, K.; Gieré, R. Risk ranking of bioaccessible metals from fly ash dissolved in simulated lung and gut fluids. *Environ. Sci. Technol.* **2005**, *39*, 7749−7756.

(11) Gray, J. E.; Plumlee, G. S.; Morman, S. A.; Higueras, P. L.; Crock, J. G.; Lowers, H. A.; Witten, M. L. In vitro studies evaluating leaching of mercury from mine waste calcine using simulated human body fluids. *Environ. Sci. Technol.* **2010**, *44*, 4782−4788.

(12) Davies, N. M.; Feddah, M. R. A novel method for assessing dissolution of aerosol inhaler products. *Int. J. Pharm.* **2003**, *255*, 175−187.

(13) Kumar, P.; Bohidar, H. B. Aqueous dispersion stability of multi-carbon nanoparticles in anionic, cationic, neutral, bile salt and pulmonary surfactant solutions. *Colloid Surf., A* **2010**, *361*, 13−24.

(14) Xing, B.; Pignatello, J. J.; Gigliotto, B. Competitive sorption between atrazine and other compounds in soils and model sorbents. *Environ. Sci. Technol.* **1996**, *30*, 2432−2440.

(15) Yang, K.; Zhu, L.; Xing, B. Adsorption of polycyclic aromatic hydrocarbons by carbon nanomaterials. *Environ. Sci. Technol.* **2006**, *40*, 1855−1861.

(16) Birch, H.; Gouliarmou, V.; Lützhøft, H. H.; Mikkelsen, P. S.; Mayer, P. Passive dosing to determine the speciation of hydrophobic organic chemicals in aqueous samples. *Anal. Chem.* **2010**, *82*, 1142−1146.

(17) Gouliarmou, V.; Smith, K. E. C.; de Jonge, L. W.; Mayer, P. Measuring binding and speciation of hydrophobic organic chemicals at controlled freely dissolved concentrations and without phase separation. *Anal. Chem.* **2012**, *83*, 1601−1608.

(18) Gross, T.; Zmora, E.; Levi-Kalisman, Y.; Regev, O.; Berman, A. Lung-surfactant-meconium interaction: In vitro study in bulk and at the air-solution interface. *Langmuir* **2006**, *22*, 3243−3250.

(19) Lin, D.; Xing, B. Tannic acid adsorption and its role for stabilizing carbon nanotube suspensions. *Environ. Sci. Technol.* **2008**, *42*, 5917−5923.

(20) Smith, K. E. C.; Dom, N.; Blust, R.; Mayer, P. Controlling and maintaining exposure of hydrophobic organic compounds in aquatic toxicity tests by passive dosing. *Aquat. Toxicol.* **2010**, *98*, 15−24.

(21) Yang, K.; Jing, Q.; Wu, W.; Zhu, L.; Xing, B. Adsorption and conformation of a cationic surfactant on single-walled carbon

nanotubes and their influence on naphthalene sorption. *Environ. Sci. Technol.* **2010**, *44*, 681−687.
(22) Xing, B. Sorption of anthropogenic organic compounds by soil organic matter: A mechanistic consideration. *Can. J. Soil Sci.* **2001**, *81*, 317−323.
(23) Kah, M.; Zhang, X.; Jonker, M. T. O.; Hofmann, T. Measuring and modeling adsorption of PAHs to carbon nanotubes over a six order of magnitude wide concentration range. *Environ. Sci. Technol.* **2011**, *45*, 6011−6017.
(24) Smith, K. E. C.; Oostingh, G. J.; Mayer, P. Passive dosing for producing defined and constant exposure of hydrophobic organic compounds during in vitro toxicity tests. *Chem. Res. Toxicol.* **2010**, *23*, 55−65.
(25) Wetterau, J. R.; Jonast, A. Effect of dipalmitoylphosphatidylcholinevesicle curvature on the reaction with human apolipoprotein A-I. *J. Biol. Chem.* **1982**, *257*, 10961−10966.
(26) Yamamoto, H.; Liljestrand, H. M. Partitioning of selected estrogenic compounds between synthetic membrane vesicles and water: Effects of lipid components. *Environ. Sci. Technol.* **2004**, *38*, 1139−1147.
(27) Park, Y.; Franses, E. I. Effect of a PEGylated lipid on the dispersion stability and dynamic surface tension of aqueous DPPC and on the interactions with albumin. *Langmuir* **2010**, *26*, 6932−6942.
(28) Fernsler, J. G.; Zasadzinski, J. A. Competitive adsorption: A physical model for lung surfactant inactivation. *Langmuir* **2009**, *25*, 8131−8143.
(29) Wiedmann, T. S.; Bhatia, R.; Wattenberg, L. W. Drug solubilization in lung surfactant. *J. Controlled Release* **2000**, *65*, 43−47.
(30) Yang, K.; Xing, B. Desorption of polycyclic aromatic hydrocarbons from carbon nanomaterials in water. *Environ. Pollut.* **2007**, *145*, 529−537.
(31) White, R. T.; Damm, D.; Miller, J.; Spratt, K.; Schilling, J.; Hawgood, S.; Benson, B.; Cordell, B. Isolation and characterization of the human pulmonary surfactant apoprotein gene. *Nature* **1985**, *317*, 361−363.
(32) Nakahara, H.; Lee, S.; Sugihara, G.; Chang, C.; Shibata, O. Langmuir monolayer of artificial pulmonary surfactant mixtures with an amphiphilic peptide at the air/water interface: Comparison of new preparations with Surfacten (Surfactant TA). *Langmuir* **2008**, *24*, 3370−3379.
(33) Agmo Hernández, V.; Karlsson, G.; Edwards, K. Intrinsic heterogeneity in liposome suspensions caused by the dynamic spontaneous formation of hydrophobic active sites in lipid membranes. *Langmuir* **2011**, *27*, 4873−4883.
(34) Wallace, E. J.; Sansom, M. S. P. Carbon nanotube self-assembly with lipids and detergent: A molecular dynamics study. *Nanotechnology* **2009**, *20*, 045101.
(35) Henriksen-Lacey, M.; Bramwell, V.; Perrie, Y. Radiolabelling of antigen and liposomes for vaccine biodistribution studies. *Pharmaceutics* **2010**, *2*, 91−104.
(36) Pan, B.; Ghosh, S.; Xing, B. Nonideal binding between dissolved humic acids and polyaromatic hydrocarbons. *Environ. Sci. Technol.* **2007**, *41*, 6472−6478.
(37) Wang, X.; Lu, J.; Xing, B. Sorption of organic contaminants by carbon nanotubes: Influence of adsorbed organic matter. *Environ. Sci. Technol.* **2008**, *42*, 3207−3212.
(38) Tsai, S.; Hofmann, M.; Hallock, M.; Ada, E.; Kong, J.; Ellenbecker, M. Characterization and evaluation of nanoparticle release during the synthesis of single-walled and multiwalled carbon nanotubes by chemical vapor deposition. *Environ. Sci. Technol.* **2009**, *43*, 6017−6023.
(39) Mueller, N. C.; Nowack, B. Exposure modeling of engineered nanoparticles in the environment. *Environ. Sci. Technol.* **2008**, *42*, 4447−4453.
(40) Plata, D. L.; Gschwend, P. M.; Reddy, C. M. Industrially synthesized single-walled carbon nanotubes: Compositional data for users, environmental risk assessments, and source apportionment. *Nanotechnology* **2008**, *19*, 185706.